Digital Restoration and Cultural and Creative Application of Ethnic Embroidery Textile Patterns Using U-Net and Texture Fusion

Xiao BAI
School of Art and Design, Henan University of Engineering, Zhengzhou 451191, Henan, China
Corresponding author: Xiao BAI (e-mail: baixiao89@126.com)

ABSTRACT Ethnic embroidery textile patterns constitute important carriers of cultural heritage; however, long-term preservation often results in fading, structural damage, and texture loss, limiting their artistic value and digital utilization. To address these challenges, this study proposes a digital restoration framework that integrates an improved U-Net convolutional neural network with adaptive texture fusion for high-fidelity embroidery pattern reconstruction. The enhanced U-Net architecture, incorporating residual connections, attention-guided skip pathways, and multi-scale feature extraction, is employed to accurately identify defective regions and recover structural information, while a PatchMatch-based texture migration strategy and VGG-guided style consistency optimization are introduced to achieve seamless texture completion and visual coherence. Furthermore, the restored patterns are transformed into reusable digital assets for cultural and creative product design, promoting the sustainable preservation and value regeneration of ethnic embroidery resources. Experimental results demonstrate that the proposed method achieves an IoU of 0.89 and a Dice coefficient of 0.88, while attaining PSNR values of 33.5–34.4 dB and superior texture consistency and visual aesthetics compared with conventional approaches. From the perspective of intelligent digital heritage systems, the proposed framework also provides technical support for multimodal information acquisition, electromagnetic-enabled sensing platforms, and wireless visualization applications, offering potential references for future integration with antenna-assisted imaging and electromagnetic data transmission technologies in smart cultural preservation environments.

INDEX TERMS u-net, texture fusion, digital image restoration, electromagnetic sensing, ethnic embroidery

I. INTRODUCTION

As an essential component of China's intangible cultural heritage, ethnic embroidery encompasses rich ethnic aesthetics, craft traditions, and historical memories, representing a critical visual carrier of China's distinguished traditional culture [1,2]. However, due to factors such as age, material fragility, and inadequate preservation environments, numerous embroidery artifacts exhibit issues including faded patterns, thread loss, partial damage, and severe deterioration [3,4]. These challenges not only hinder the comprehensive presentation of their historical and artistic value but also impede subsequent digital preservation, cultural transmission, and creative development [5,6]. Consequently, achieving efficient, realistic, and controllable digital restoration of ethnic embroidery patterns has become a focal topic in contemporary research on the digital safeguarding of intangible cultural heritage [7,8].

Traditional pattern restoration predominantly relies on hand-painting, manual repair, or semi-automatic methods utilizing image processing software [9,10]. Such techniques are inefficient, demand substantial professional expertise from operators, and lack scalability for processing large datasets [11,12].

Technologically, existing algorithms present several key limitations: first, they often fail to accurately recognize pattern structures, leading to structural distortion in restoration outcomes [13,14]; second, they exhibit limited capabilities in reconstructing texture information, making it difficult for restored areas to blend naturally with the original image in terms of texture and color [15]; third, they lack a unified automated workflow, hindering the efficient transformation of restoration results into standardized pattern materials suitable for cultural and creative design [16]. Therefore, there is an urgent need to adopt intelligent restoration methods that integrate structural learning and texture modeling capabilities to achieve high-fidelity, automated digital restoration of ethnic patterns [17].

Recent advancements in deep learning have significantly impacted the field of image restoration [18]. For instance, Wang et al. [15] explored pathways for cultural sustainability in traditional clothing embroidery patterns through digital generative art. Sha et al. [19] proposed combining the YOLOv4–ViT (You Only Look Once version 4 – Vision Transformer) collaborative recognition network with an enhanced generative adversarial network to facilitate efficient classification and restoration of ancient textile images. In response to the limitations of traditional pattern restoration, some studies have attempted to apply methods such as style transfer and generative adversarial networks for intelligent pattern filling and reproduction [20,21].

However, these approaches primarily address natural images or oil painting styles. For ethnic embroidery patterns characterized by intricate structures and highly repetitive textures, challenges such as missing restoration details, unnatural texture fusion, and distorted style outcomes persist. Furthermore, most existing studies have not effectively integrated image restoration results with the development of cultural and creative products, limiting the transformation of cultural resources and practical industrial implementation [22].

To address these issues, this paper proposes a digital restoration method for ethnic embroidery patterns based on a U-Net deep convolutional neural network and an adaptive texture fusion algorithm. First, an improved U-Net network architecture is constructed, facilitating structural reconstruction of defective areas within embroidery patterns through up-sampling, down-sampling, and a skip connection mechanism. Next, the PatchMatch texture migration strategy is utilized to guide and complete the texture style of the restored area, ensuring natural visual transitions between the restoration result and the original image. Building on this, the restored pattern outcomes are applied to the development of digital cultural and creative products, realizing a technical closed-loop from "pattern restoration" to "cultural redesign."

II. AUTOMATIC RECONSTRUCTION OF PATTERN STRUCTURE AND FUSION OF TEXTURE DETAILS

A. AUTOMATIC IDENTIFICATION OF DEFECTIVE AREAS IN EMBROIDERY PATTERNS

In the digital restoration of ethnic embroidery patterns, precise identification of defective areas is fundamental to effective reconstruction and texture fusion. Given the blurred edges, irregular shapes, and complex texture backgrounds characteristic of damaged embroidery regions, this paper introduces an image segmentation network based on an improved U-Net architecture to automatically identify damaged areas and generate binary masks. The overall network structure adheres to the symmetric encoder–decoder design of the classic U-Net, enabling the transmission and restoration of spatial features into semantic information through five layers of convolutional downsampling and five layers of upsampling deconvolution. To enhance recognition of small-scale damaged details, the encoder incorporates a residual connection structure following each convolutional layer, with identity mapping added after two layers of 3×3 convolution and ReLU activation. This approach effectively mitigates the vanishing gradient problem and improves feature stability and training efficiency. Each residual block is followed by 2×2 max pooling for downsampling, progressively expanding the receptive field. The structure is illustrated in Figure 1.

Figure 1 depicts a two-layer residual block combined with pooling, which is employed to extract texture, edge, and structural features from the image's lower to middle layers. In the restoration of ethnic embroidery patterns, details such as yarn edges and breaks in complex patterns are often minute, requiring a high level of recognition by the model. Standard convolutions may overlook such minor damage, whereas residual connections facilitate the network's ability to learn variations in these fine regions, making the model particularly suited for restoring images with high texture density, such as embroidery patterns.

Regarding the skip connection mechanism, the traditional U-Net directly concatenates feature maps from corresponding layers in the decoder stage. To enhance boundary information retention and feature matching accuracy, this paper adopts attention-gated skip connections. This mechanism suppresses background redundancy via a lightweight attention module, which calculates gated attention weights prior to concatenation, thereby improving semantic alignment in damaged areas.

Additionally, to address the coexistence of blurred texture boundaries and multi-scale damage in embroidery patterns, dilated convolution replaces certain standard convolutions, expanding the receptive field without increasing parameter count. This enables the model to capture large-scale defect contours while retaining small-area details. The encoder's final feature map is extracted using a parallel dilated convolution module (dilation rates of 1, 2, and 4), and dimensions are unified via a channel compression module. For the damaged area segmentation task, the training objective utilizes a weighted Dice loss function in combination with binary cross-entropy loss. Given that defective regions in embroidery patterns are typically small and feature complex edges, relying solely on cross-entropy may result in regional prediction bias. Therefore, the Dice loss is employed to enhance the model's sensitivity to regional overlap. The formula is as follows:

$$\mathcal{L} = \alpha \cdot \mathcal{L}_{\text{Dice}} + (1 - \alpha) \cdot \mathcal{L}_{\text{BCE}}, \quad \alpha = 0.7 \tag{1}$$

Here, $\mathcal{L}_{\text{Dice}}$ loss increases the model's sensitivity to overlap between predicted and actual regions, while $\mathcal{L}_{\text{BCE}}$ loss addresses pixel-wise classification. The coefficient α serves as a weighting factor to balance the contributions of these two loss components.

During data preprocessing, collected ethnic embroidery image samples are standardized and cropped to a uni-

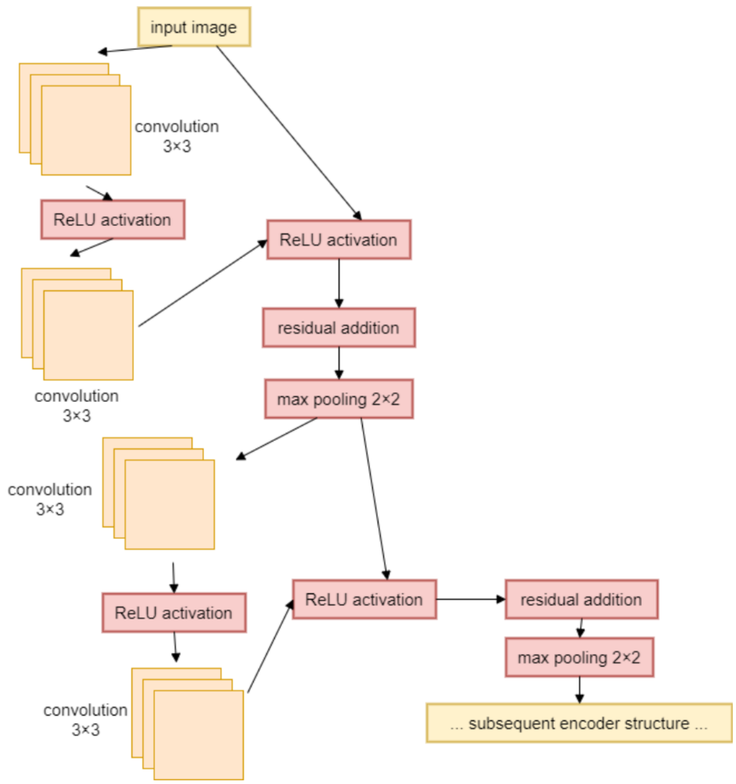

FIGURE 1. Residual connection structure application

form resolution of 256×256 pixels. Defective areas are manually annotated as ground truth. Subsequently, image augmentation techniques such as rotation, flipping, and color perturbation are applied to enhance model robustness and prevent overfitting.

The training process employs the Adam optimizer with a learning rate of 1×10^{-4}, cosine annealing scheduling, a batch size of 16, and 150 training epochs. The output is a binary mask that highlights damaged areas, ensuring precise inputs for structural reconstruction and texture fusion.

The framework addresses the needs of three stakeholders: cultural heritage experts, textile conservators, and digital designers. Restored patterns are exported in .SVG and .PNG formats for seamless integration with conservation databases and design tools. The architecture is tailored for ethnic embroidery restoration through three key features: residual blocks for micro-damage retention, attention gates for boundary feature emphasis, and parallel dilated convolutions (rates 1, 2, and 4) for multi-scale context capture. This design enhances feature representation and distinguishes itself from general-purpose U-Net models.

B. STRUCTURAL RECONSTRUCTION OF DEFECTIVE AREAS

For damaged masked areas in embroidery patterns, this paper proposes a context-aware reconstruction mechanism based on a U-Net decoder to restore structural details. The model encodes the input image and the masked area as parallel channels, extracting both context and defect constraint features. Following the encoding stage, the decoder restores resolution through stepwise upsampling, incorporating skip connections filtered by an attention mechanism to ensure semantic consistency with the damaged regions. A multi-scale context fusion structure is integrated into the U-Net decoder to enhance structural restoration.

High-order feature maps are processed through three parallel paths: a standard 3×3 convolution for medium-scale features, a dilated convolution (rate = 2) for large-area context, and a 1×1 convolution for global semantic compression. These outputs are fused using channel-wise attention to suppress irrelevant information and emphasize pattern outlines and texture boundaries. The enhanced features guide the decoder, enabling accurate structural completion and fine restoration.

Table 1 compares different convolution structures in terms of parameter count and computational complexity.

The standard U-Net has fewer parameters and lower complexity but limited receptive fields, rendering it insufficient for complex embroidery restoration. The 1×1 convolution reduces computation while retaining global low-dimensional features. The multi-scale context fusion structure, which combines three convolution types, improves restoration robustness and performance with only a slight increase in parameters and computation. Inference latency is 0.41 s per 256×256 image on an NVIDIA RTX A5000 GPU and 9.2 s per image on an Intel Core i7-12700H CPU using ONNX Runtime, supporting heritage digitization workflows.

TABLE 1. Parameter quantity and computational complexity under different convolution methods

Model Configuration	Convolution Type	Perceptual Range	Parameter Count (Million)	Computational Complexity (FLOPs)
Standard U-Net	3×3 Convolution	Medium-scale local structure	10.2	6.1 B
U-Net with Dilated Convolution	Dilated Convolution ($d = 2$)	Large-area context perception	11.5	6.5 B
U-Net with 1×1 Convolution	1×1 Convolution	Retains global low-dimensional representation	9.8	5.8 B
Multi-Scale Context Fusion	3×3 + Dilated ($d = 2$) + 1×1	Fusion of medium- to large-scale and global low-dimensional information	12.1	6.9 B

To exploit symmetry and repetitive patterns, a spatial self-attention module in the decoder matches non-local features, enhancing long-distance structural correlations for continuous pattern recovery. A structural residual fusion mechanism is applied after the final convolution, fusing the predicted structure map with high-resolution edge maps from the encoder. This ensures edge continuity, symmetry, and faithful restoration of pattern contours.

Regarding loss function design, this paper does not use a single pixel loss but constructs a combined loss function to comprehensively measure the geometric consistency and local accuracy of structure recovery, as follows:

$$\mathcal{L}_{\text{recon}} = \lambda_1 \cdot \mathcal{L}_{L1} + \lambda_2 \cdot \mathcal{L}_{\text{Perceptual}} + \lambda_3 \cdot \mathcal{L}_{\text{SSIM}} \quad (2)$$

$\mathcal{L}_{L1}$ guarantees pixel-level accuracy. $\mathcal{L}_{\text{Perceptual}}$ extracts semantic features based on the intermediate layers of the VGG-19 (VGG 19-layer network) to maintain high-level structural consistency. $\mathcal{L}_{\text{SSIM}}$ loss is used to enhance texture continuity and spatial consistency between local structures. The parameters are set to $\lambda_1 = 0.5$, $\lambda_2 = 0.3$, $\lambda_3 = 0.2$ optimized values. Experimental validation demonstrates that this configuration achieves optimal performance in both visual subjective scoring and structural indicators. Additionally, to avoid overfitting to structural priors, the training samples employ a pseudo-defect simulation mechanism that randomly generates occlusion areas in the original image, conforming to the morphological characteristics of embroidery patterns. This approach ensures a balanced coverage distribution of various shapes, sizes, and positions, thereby improving the model's generalization capability for real damage scenarios.

For artifacts lacking a complete reference, $\mathcal{L}_{\text{Perceptual}}$ transfers style knowledge from intact regions to damaged ones. The model establishes local style consistency by correlating texture features within preserved pattern fragments. This self-referential approach enables reconstruction without relying solely on ground truth.

C. TEXTURE FEATURE MIGRATION AND FUSION

After structural reconstruction, the generated embroidery pattern is complete but lacks fine texture and color variation, resulting in style discontinuities. To enhance naturalness, a texture feature migration mechanism based on the PatchMatch algorithm is applied. Texture blocks are extracted from valid areas of the original image or from an external database to guide precise texture completion and style transition. The restored area is first located using the structural mask as an initial guide. Reference blocks are extracted from the surrounding neighborhood via a sliding window to form a candidate set. PatchMatch then iteratively searches for the best match, propagating offsets from adjacent blocks and applying random perturbations within a narrowed range to optimize texture alignment.

Table 2 presents the performance and convergence of PatchMatch-based texture synthesis over 10 iterations.

The average matching error (pixel difference) decreases from 12.5 to 2.8, indicating steadily improving match quality and more natural texture fusion. The offset vector update rate drops from 45% to 0.5%, reflecting rapid convergence and stabilization of matching results. Runtime per iteration remains stable at 0.26–0.35 s, demonstrating high efficiency suitable for practical applications.

TABLE 2. Iterative performance

Iteration	Average Matching Error (pixels)	Offset Vector Update Rate (%)	Runtime (seconds)
1	12.5	45	0.35
2	8.7	30	0.32
3	6.1	20	0.31
4	4.5	12	0.3
5	3.8	8	0.29
6	3.2	5	0.28
7	3	3	0.27
8	2.9	2	0.27
9	2.8	1	0.26
10	2.8	0.5	0.26

The texture block similarity measurement function, based on the L2 norm, is used to calculate the matching error, with the smallest value selected as the current optimal match.

$$D(p, q) = \|I_p - I_q\|_2^2 + \beta \cdot \|G_p - G_q\|_2^2 \quad (3)$$

where I_p and I_q are the color value matrices of the current and candidate blocks, respectively; G_p and G_q are their gradient information (to maintain consistent texture direction); and β is the balance coefficient, set to 0.3 in the experiment.

Following PatchMatch-based block matching, the best texture blocks are copied to the restoration area. To prevent edge artifacts and gaps, a minimum graph cut is applied: an energy map of overlapping regions considers texture gradients and color differences, and the cut with minimum cost defines a smooth fusion boundary. This process ensures seamless transitions between blocks. After block-level synthesis, a global texture adjustment is performed using a guide map derived from the gradient and local color histogram. A local weighted residual smoothing algorithm refines color and texture across the restoration area for uniformity. Candidate texture blocks are normalized in color space and processed with principal component analysis to retain the main texture directions, remove low-energy or redundant components, and enhance detail retention, consistency, and naturalness in the final result.

The texture synthesis strictly samples from authenticated regions of the original artifact. A maximum displacement threshold confines patch retrieval to geometrically congruent zones. This constraint preserves structural authenticity while preventing statistically driven fabrications.

D. STYLE CONSISTENCY OPTIMIZATION AND CULTURAL AND CREATIVE PATTERN REUSE

After structural reconstruction and texture fusion, the overall pattern is restored in physical form. However, due to differences in restoration paths and feature generation methods across regions, local deviations between the restoration area and the original pattern persist, primarily manifesting as color style drift, inconsistent texture scales, and uneven brushstroke intensity. To address these issues, this paper applies a style loss function based on the output of the visual geometry group (VGG) network perception layer to fine-tune consistency, ensuring the entire image is unified in texture granularity, color saturation, and decorative style.

Style consistency optimization preserves intentional compositional features while tolerating natural variations. The gram matrix loss operates on low-frequency texture distributions, excluding high-frequency stochastic details characteristic of handmade execution. A perturbation term (σ = 0.15) introduces controlled randomness within the original texture parameters, preventing artificial homogeneity.

The image I_{output} that has undergone structural reconstruction and texture migration is used as a candidate restoration image. It is input, together with the style reference image I_{ref} extracted from undamaged regions of the original image, into the pre-trained VGG-19 network. Feature response maps are extracted from the following layers of the pre-trained VGG-19 network: conv1_1, conv2_1, conv3_1, conv4_1, and conv5_1. For each layer output, the corresponding Gram matrix is constructed to measure its style distribution:

$$ {}_{ij}G^l = \sum_k {}_{ik}F^l \cdot {}_{jk}F^l \tag{4} $$

where F^l is the feature map of the l-th layer, and G^l represents the gram matrix for that layer. The correlation between channels is obtained by calculating the inner product between pixels in the channel, reflecting the texture style characteristics. The sum of the squares of the gram matrix differences between the restoration image and the reference image at each layer is used as the style loss:

$$ \mathcal{L}_{\text{style}} = \sum_l \omega_l \cdot \|G_l(I_{\text{output}}) - G_l(I_{\text{ref}})\|_F^2 \tag{5} $$

where ω_l is the loss weight for each layer, which is set to decrease from shallow to deep, thereby strengthening the style consistency of the underlying texture. The optimization objective is to minimize the loss function, and the Limited-memory Broyden–Fletcher–Goldfarb–Shanno (L-BFGS) algorithm is used to iteratively update the image pixels to achieve style domain alignment. To further avoid excessive homogenization of restoration area details, this paper jointly applies a content preservation term, using the output of the conv4_1 layer in the VGG network as the content constraint to maintain stable pattern semantic structure while adjusting only the style distribution. The final joint optimization objective function is:

$$ \mathcal{L}_{\text{total}} = \lambda_1 \cdot \mathcal{L}_{\text{style}} + \lambda_2 \cdot \mathcal{L}_{\text{content}} \tag{6} $$

In the experiment, $\lambda_1 = 1.0$, $\lambda_2 = 0.3$ are set, and the style is the core optimization direction, while ensuring that the structural content does not drift. After completing the fine-tuning of style consistency, the overall image tone, texture scale, and local brushstroke form tend to be unified. Subsequently, the final restoration pattern is exported to the cultural and creative pattern element design module to perform pattern reuse operations.

In the experiments, $\alpha = 0.7$ in Eq. 1; $\lambda_1 = 0.5$, $\lambda_2 = 0.3$, $\lambda_3 = 0.2$ in Eq. 2; and $\lambda_1 = 1.0$, $\lambda_2 = 0.3$ in Eq. 6. These hyperparameter values result from systematic grid search experiments. The optimization objective balances pixel accuracy (L1/L2), perceptual consistency (VGG-based loss), and structural integrity (SSIM). Parameter combinations are evaluated on a validation set of 50 embroidery images with varying damage patterns. The selected values maximize joint performance across PSNR and SSIM metrics while avoiding modality dominance.

The restored patterns undergo digital adaptation for materialization in product design contexts. Standardized transformations—tiling, mirroring, and contour extraction—generate base pattern derivatives. These derivatives serve as modular assets compatible with computer-aided design systems. This process reduces manual vectorization labor while preserving indigenous motif structures. Design teams subsequently refine these assets within professional workflows, integrating cultural narratives and market-specific aesthetics.

The restoration image is layer-segmented according to color distribution and texture boundaries; independent pattern elements are extracted; and vectorized layer files are generated to ensure suitability for subsequent product size scaling and pattern deformation operations. The pattern arrangement system, based on shape matching, is then used to automatically generate derivative versions such as tiled styles, symmetrical patterns, and outline silhouettes in the pattern library, expanding the application range in printing design, embroidery patterns, and ribbon patterns. The automatic generation process is illustrated in Figure 2.

Figure 2 displays the visual effects of the same ethnic embroidery pattern elements after processing in three different arrangement styles. Tiling involves repeating the original pattern horizontally and vertically to create a continuous, seamless background pattern. This arrangement is suitable for fabric printing and large-area decoration, ensuring overall continuity and repeatability and facilitating large-scale production. Mirror symmetry uses a combination of horizontal and vertical flipping to arrange the pattern symmetrically, enhancing visual rhythm and structural beauty. This method retains local pattern details while enhancing design layering through symmetry, making it suitable for embroidery plate and ribbon design. The silhouette outline is generated by edge extraction and smoothing, resulting in a clear outline of the pattern and highlighting the shape characteristics of the embroidery elements. This style is suitable as a design element in cultural and creative products, such as a simplified pattern symbol for printing, logos, or digital pattern libraries, and is convenient for secondary creation and style extension.

Once the restoration work is complete, the next step is to integrate the restored embroidery patterns into modern design and cultural product development processes.

The fusion of traditional cultural elements with modern creative expression plays a key role in the preservation and revitalization of ethnic heritage. Thanks to the high-quality restoration results achieved by this method, the restored patterns can be further customized. Designers can manipulate the digital files of the embroidery and incorporate them into product designs such as textiles, clothing, wallpaper, or decorative items. Furthermore, the digital nature of the restored embroidery enables interactive design. Designers can apply transformations such as color adjustments, pattern scaling, or abstract modifications while maintaining a direct connection to the original design. This opens up new possibilities for creating personalized cultural products that blend traditional and modern elements.

Beyond physical products, the digital restoration of ethnic embroidery patterns facilitates their integration into digital media such as video games, virtual reality environments, and interactive installations. By preserving their rich textures and consistent style, these patterns can become part of immersive experiences, celebrating and promoting cultural heritage in modern digital forms. Preserving traditional embroidery through digital restoration also allows for its use in augmented reality and 3D rendering projects, where the patterns can be projected into various environments. This further enhances the cultural value of the design and provides users with a unique and interactive way to engage with traditional art.

III. EVALUATIONS

The experimental parameters include PatchMatch iterations: 10; U-Net model input size: 256×256; batch size: 16; optimizer: Adam; initial learning rate: 1×10^{-4}; weight decay: 1×10^{-5}. The test dataset uses a selfbuilt embroidery pattern defect restoration dataset, which contains 500 sets of images, divided into training sets (400) and test sets (100). The dataset encompasses 15 ethnic groups with distinct embroidery styles, including Miao cross-stitch, Zhuang brocade, and Uyghur floral motifs. Damage types cover thread breakage (38%), color fading (29%), partial missing areas (22%), and contaminant stains (11%). Pattern complexity ranges from geometric primitives (120 samples) to figurative scenes (230 samples) and hybrid compositions (150 samples), with damaged areas occupying 5–60% of the total pattern space.

A. STRUCTURAL RECONSTRUCTION ACCURACY

The accuracy and completeness of the structural reconstruction method based on the improved U-Net decoder, combined with multi-scale feature fusion in the restoration of defective areas in ethnic embroidery patterns, are verified. The experimental data selects embroidery pattern images with marked defective areas, including various defect types (fading, damage, missing). The real lossless pattern corresponds to the complete lossless image of the same pattern, serving as the reference for structural reconstruction. The damaged image is input into the improved U-Net model to obtain the reconstructed, complete embroidery pattern structure. The reconstruction area is located using the defective area mask, and only the accuracy of the defective part is evaluated. The pixel-level overlap between the reconstructed area and the real lossless area is calculated using the following indicators: Intersection over Union (IoU) and Dice coefficient. At the same time, the structural reconstruction accuracy of each method is compared, and the mean and standard deviation of the results of multiple groups of samples are calculated. “Traditional inpainting” refers to the PatchMatch algorithm for image completion.

Figure 3 compares the structural accuracy of various embroidery pattern restoration methods using IoU and Dice coefficients. The traditional method performs worst (IoU: 0.65, Dice: 0.60), while our proposed U-Net-based method with texture fusion achieves the highest scores (IoU: 0.89, Dice: 0.88), demonstrating superior structural restoration. Error bars indicate stability: traditional methods fluctuate most, whereas our method shows minimal variation, reflecting strong robustness. Incorporating texture fusion notably improves performance over U-Net alone, emphasizing its role in maintaining pattern continuity. Comparisons with EdgeConnect, LaMa, CoModGAN, and MAT show that our method consistently achieves the highest accuracy and stability across diverse defect types.

B. PEAK SIGNAL-TO-NOISE RATIO

Damaged images containing ethnic embroidery patterns and corresponding lossless reference images are prepared to ensure that the data covers a variety of pattern types and damage levels. The damaged images and reference images

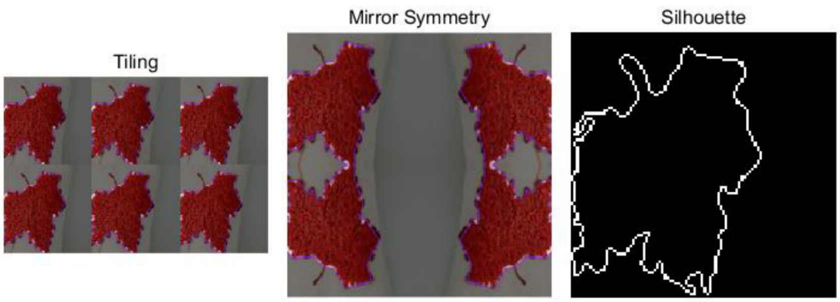

FIGURE 2. Different arrangement styles

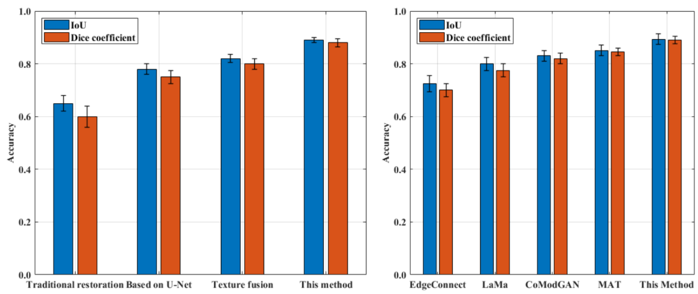

FIGURE 3. Structural accuracy performance of various embroidery pattern repair methods

are resized, converted to color space, and normalized to ensure that the input data is consistent. Four restoration methods—traditional restoration, U-Net-based restoration, restoration based on U-Net plus texture fusion, and the method proposed in this paper—are used to restore the damaged images and generate corresponding restoration results. The peak signal-to-noise ratio (PSNR) is calculated pixel by pixel for each restoration result and its corresponding lossless reference image, and the PSNR values of each method on all test samples are summarized. The mean and standard deviation are calculated to evaluate the fidelity and stability of the restoration effect.

The PSNR is calculated between each restored image and its corresponding lossless reference across the entire test set of 100 samples. The average PSNR values and standard deviations for the four methods are as follows: traditional restoration (29.4 $\pm$ 0.8 dB), U-Net-based (31.0 $\pm$ 0.6 dB), texture fusion (32.8 $\pm$ 0.5 dB), and this method (33.9 $\pm$ 0.4 dB).

Figure 4 visually depicts the PSNR trends for a subset of 10 representative samples, illustrating the consistent performance advantage of the proposed method across varied pattern types and damage severities. The horizontal axis is the image sample number, and the vertical axis is the PSNR value (unit: dB), which is used to measure the fidelity of image restoration. The overall PSNR level of traditional restoration is the lowest, with values concentrated in the 28.5–30.2 dB range, indicating that the restoration results of this method are quite different from the original image, with poor fidelity and some fluctuations. The U-Net-based method shows significant improvement over the traditional method, with PSNR stable in the range of 30.2–31.5 dB, demonstrating enhanced structural restoration capabilities. Texture fusion (U-Net + texture fusion) further improves the overall quality, with PSNR reaching 32.1–33.4 dB and smaller fluctuations, indicating that the restoration area is more consistent with the real image after the application of texture information. This method achieves the highest PSNR (33.5–34.4 dB) among all samples, showing stronger image fidelity and small value fluctuations, indicating good generalization ability and stability across multiple pattern types.

C. STRUCTURAL SIMILARITY INDEX

Image samples of ethnic embroidery patterns with defects and the corresponding lossless reference images are collected. The number of samples is sufficient to ensure statistical significance. For each defective image, four restoration methods are used: traditional restoration, U-Net-based structural reconstruction, restoration with texture fusion, and the comprehensive restoration method combining multi-scale context fusion and texture fusion proposed in this paper. The structural similarity index is calculated for each restoration result and the corresponding lossless reference image to measure visual quality and structural coherence. Figure 5 shows the distribution of the structural similarity index for the four restoration methods across all test samples, evaluating the visual quality and texture consistency of each

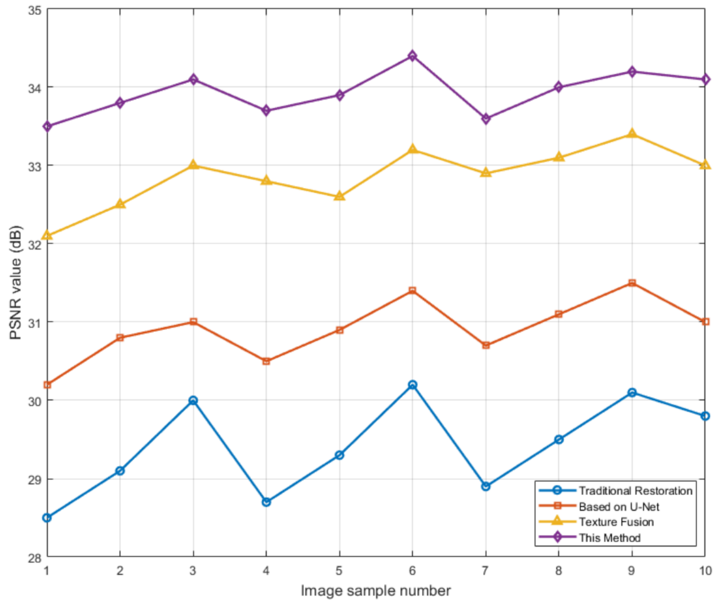

FIGURE 4. Peak signal-to-noise ratio performance across a representative subset of 10 test samples

method. The horizontal axis represents the four restoration methods, and the vertical axis is the structural similarity index measure (SSIM), ranging from 0.7 to 1. The SSIM distribution of the traditional method is low, and the median and overall concentration are lower than those of other methods, indicating that its restoration effect is relatively poor and its stability is low. The U-Net-based method improves upon this, with an increased SSIM mean, indicating enhanced structural reconstruction ability. The texture fusion method further improves SSIM, showing that texture details and overall visual quality are better maintained. The method proposed in this paper performs best on the SSIM index and shows the highest median, indicating that its restoration results are superior in terms of visual quality and texture consistency.

D. TEXTURE CONSISTENCY INDEX

The restoration image of the ethnic embroidery pattern containing the defective area and its corresponding original lossless reference image are collected. The mask of the restoration area is determined for subsequent positioning of texture feature extraction. The grayscale co-occurrence matrix and local binary pattern texture features are extracted from the restoration area and its neighborhood, respectively. Various texture description metrics are calculated, including contrast, correlation, energy, and homogeneity. The texture features of the restoration area are compared with those of the neighboring reference area, and the texture consistency scores for each index are obtained using the similarity calculation method. For each test image, the texture consistency index of the four restoration methods is calculated separately. The texture consistency index of all test images is summarized. The texture consistency performance of different restoration methods is compared, and a significance analysis is performed.

The bar chart on the left of Figure 6 shows the specific scores of the four restoration methods on the four texture consistency indicators: contrast, correlation, energy, and homogeneity. "This method" performs best in all four indicators, especially in contrast and energy, indicating that it is better at maintaining texture contrast and energy. The traditional method scores the lowest, indicating that its texture restoration ability is weak. The performance of the U-Net and Texture Fusion methods gradually improves, showing the benefits brought by texture fusion technology. The line chart on the right shows the average texture consistency score of each method, and "This Method" has the highest average score, indicating that its overall texture consistency is the best. The traditional method scores the lowest and performs the weakest.

E. VISUAL AESTHETIC EVALUATION

Embroidery pattern samples processed by different restoration methods are selected, including traditional methods, U-Net-based methods, texture fusion methods, and the method proposed in this paper. A scoring questionnaire with five indicators—color coordination, texture details, artistic sense, color distribution consistency, and edge clarity—is designed. Each indicator is scored using a Likert scale (1–10 points). The scorers include 10 embroidery experts, 10 designers, and 10 ordinary user representatives, to take into account both professionalism and public perception. The subjective scoring data is summarized, and outliers are eliminated. The average score and standard deviation of each method and

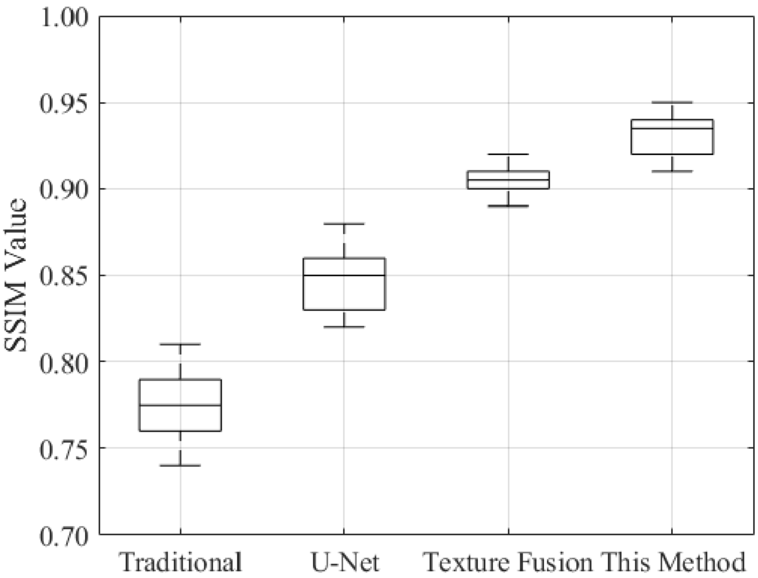

FIGURE 5. Structural similarity index

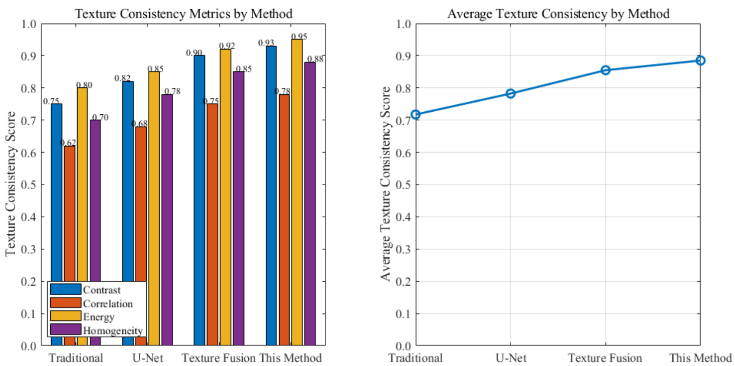

FIGURE 6. Texture consistency index

indicator are calculated.

Scoring follows a standardized protocol: assessors receive neutral instructions describing only the assessment objectives, without methodological details. Images are displayed in a randomized order on a calibrated 50-inch monitor at a viewing distance of 2 meters, with ambient lighting maintained at 500 lux D65. All results are anonymized. Each assessor independently evaluates all samples in a separate session.

Figure 7 shows the comprehensive performance of four image restoration methods on five visual aesthetic evaluation indicators: color coordination, texture details, artistic sense, color distribution consistency, and edge clarity. The four curves correspond to the traditional restoration method, the U-Net-based method, the texture fusion method, and the method proposed in this paper. The coverage area and shape of the curve reflect the performance and balance of each method on each indicator. The proposed method has high scores in all indicators, and the curve coverage area is the largest, indicating that its restoration pattern is better than those of other methods in terms of visual aesthetics. The traditional method has a low score, indicating that its visual effect is insufficient and lacks consistency and detailed performance. The method based on U-Net and texture fusion has improved in color and texture details, but is still slightly inferior to the proposed method, showing the advantages of the proposed method in comprehensive visual effect optimization.

The limited evaluator cohort constrains statistical generalizability. This preliminary assessment focuses on directional insights rather than definitive conclusions. The statistical consistency indicators are shown in Table 3.

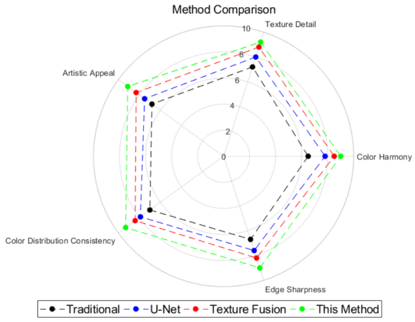

FIGURE 7. Visual aesthetic evaluation

TABLE 3. Statistical consistency

Method	Kendall's W	ICC
Traditional	0.85	0.91
U-Net	0.87	0.92
Texture Fusion	0.89	0.94
This Method	0.90	0.95

ICC, intraclass correlation coefficient.

Table 3 presents the statistical consistency metrics for the four repair methods, including Kendall's W coefficient and ICC values, which measure the consistency of ratings given by different evaluators (experts, designers, and general users). The proposed method performed best among the four methods, showing the highest consistency in ratings, which suggests that it offers the most stable and reliable repair quality.

F. HYPERPARAMETER SENSITIVITY ANALYSIS

Ablation studies validate the weighting choices in the combined loss function. For Equation 2 (structural reconstruction loss), Table 4 reports the restoration quality under variations in λ_1, λ_2, and λ_3. When λ_1 (L1 weight) exceeds 0.7, the PSNR improves, but texture continuity degrades due to pixel overfitting. Lowering λ_2 (perceptual loss weight) below 0.2 leads to semantic distortion in complex patterned areas. The selected configuration (0.5/0.3/0.2) achieves the best balance. Similar experiments guide the weighting assignments for Equations 1 and 6, where $\alpha = 0.7$ maximizes the Dice value for small defects, while $\lambda_1/\lambda_2 = 1.0/0.3$ maintains a style-content balance.

TABLE 4. Structural reconstruction quality under loss weight variations

λ_1	λ_2	λ_3	PSNR (dB)	SSIM
0.8	0.1	0.1	32.9	0.81
0.7	0.2	0.1	32.6	0.83
0.5	0.3	0.2	32.8	0.86
0.3	0.5	0.2	31.7	0.85
0.2	0.6	0.2	31.1	0.81

PSNR, peak signal-to-noise ratio; SSIM, structural similarity index measure.

G. REUSE OF CULTURAL AND CREATIVE PRODUCTS

A task-based study of professional designers evaluated the usability of restored patterns in the design process.

Twelve designers specializing in ethnic cultural products were recruited. Each designer completed a series of standardized tasks using restored digital resources, applying provided patterns to clothing and home décor templates. The task completion time and the number of manual modifications required for each pattern were quantified. After completing the tasks, designers completed a standardized usability questionnaire, rating the quality, ease of use, and style fidelity of the provided patterns. The results are shown in Table 5.

TABLE 5. Reuse of cultural and creative products

Metric	Unit	Restored Patterns (Mean)	Manual Reference Patterns (Mean)	Standard Deviation
Task Completion Time	Minutes per Pattern	15.2	21.1	2.8
Number of Modifications	Times per Pattern	1.4	2.0	0.6
Usability Score – Quality	5-Point Scale	4.6	3.8	0.3
Usability Score – Ease of Use	5-Point Scale	4.5	3.9	0.4
Usability Score – Stylistic Fidelity	5-Point Scale	4.7	4.2	0.3

The results showed that the restored patterns demonstrated high practicality, with an average 28% reduction in task completion time, a lower average revision frequency, and high scores across all usability dimensions compared to manually restored reference patterns. This evaluation provides empirical evidence for the effectiveness of digital restoration results in downstream cultural and creative applications.

H. ACTUAL APPLICATION COST

A quantitative evaluation of application costs was conducted to assess the practical deployment effectiveness of the proposed pipeline. The computational cost of training the improved U-Net model on a single NVIDIA RTX A5000 GPU was approximately 28 hours. The inference cost for repairing a single 256 × 256 image was 0.41 seconds, enabling rapid processing for collection digitization projects. Labor costs primarily involved the initial data annotation phase. Professional annotators took an average of 5 minutes to segment the defective regions in each high-resolution embroidery image, resulting in a total annotation effort of approximately 42 hours for a dataset of 500 images. This one-time cost translates into a reusable model, amortizing the cost across future restoration tasks. For cross-institutional deployment, the trained model was successfully converted to the ONNX format. It demonstrated stable performance on a common CPU-only workstation (Intel Xeon E5-2680 v4), achieving an average inference time of 9.2 seconds per image, demonstrating its deployment without the need for dedicated GPU hardware. Experimental results are shown in Table 6.

TABLE 6. Actual application cost

Metric	Unit	Value
Model Training Time	Hours	28
Inference Time (GPU)	Seconds per Image	0.41
Inference Time (CPU)	Seconds per Image	9.2
Manual Annotation Time	Minutes per Image	5
Total Annotation Effort	Hours	42

IV. CONCLUSION

This paper addresses the problem of restoring damaged ethnic embroidery textile patterns during digital preservation. An image restoration method is proposed that integrates an improved U-Net network with the PatchMatch texture synthesis algorithm, combined with a VGG style consistency optimization strategy, to achieve a complete workflow from structural reconstruction and texture transition to style coordination.

Experiments demonstrate that this method outperforms traditional methods in terms of restoration accuracy, texture naturalness, and visual consistency, demonstrating its high practical value. Furthermore, this paper further embeds the restoration results into the cultural and creative product design process to promote the revitalization and reuse of ethnic patterns. Ethnic embroidery often requires high-resolution and large-format work. Future research could optimize the model's computational efficiency and memory management to enable rapid restoration of higher-resolution images or entire fabrics while preserving structural and texture details.

AUTHOR CONTRIBUTIONS

All work in this study was independently completed by Xiao BAI.

CONFLICTS OF INTEREST

The author declares no conflict of interest.

FUNDING

This study was supported by the Key Research Project of Higher Education Institutions in Henan Province (Soft Science): "Research on the Development and Practical Strategies of Digital Products for Rural Culture and Tourism in Henan Province" (NO. 24B535001).

ACKNOWLEDGEMENTS

Not applicable.

REFERENCES

[1] N. Singh and M. Singh, "Traditional embroidery revival for sustainability: a systematic literature review and bibliometric analysis," Discover Sustainability, vol. 6, no. 1, pp. 180, 2025, doi: 10.1007/s43621-025-00944-0.

[2] X. Zhuo, D. Huang, Y. Lin, and Z. Huang, "Combined query embroidery image retrieval based on enhanced CNN and blend transformer," Scientific Reports, vol. 14, no. 1, Art. no. 27518, 2024, doi: 10.1038/s41598-024-79012-y.

[3] K. Liu, J. Zhao, and C. Zhu, "Research on Digital Restoration of Plain Unlined Silk Gauze Gown of Mawangdui Han Dynasty Tomb Based on AHP and Human–Computer Interaction Technology," Sustainability, vol. 14, no. 14, pp. 8713, 2022, doi: 10.3390/su14148713.

[4] X. M. Chen, R. D. Rusli, R. Zur, and J. Bai, "Cultural Influences on Han Chinese Embroidery Patterns during the Late 19th and Early 20th Centuries," Environment-Behaviour Proceedings Journal, vol. 10, no. 32, pp. 41-48, 2025, doi: 10.21834/e-bpj.v10i32.6698.

[5] J. Wu, X. Tan, and D. Peng, "Research on the Innovative Design of Dechang Lisu Embroidery Pattern on Plant Leather Bag," Leather Science and Engineering, vol. 34, no. 5, pp. 99-106, 2024, doi: 10.19677/j.issn.1004-7964.2024.05.014.

[6] C. Liu, J. Gu, L. Yao, and Y. Zhang, "Research on embroidery style migration model based on texture cycle GAN," International Journal of Clothing Science and Technology, vol. 37, no. 1, pp. 138-153, 2025, doi: 10.1108/IJCST-04-2023-0062.

[7] M. Yue, R. C. Me, Y. Li, and R. W. O. K. Rahmat, "Developing a metadata elements set for digital archives of Chinese restoration techniques: A scoping literature review," Multidisciplinary Reviews, vol. 8, no. 8, Art. no. e2025243, 2025, doi: 10.31893/multirev.2025243.

[8] B. Hu and S. Wang, "Digital restoration of traditional huizhou clothing based on 3D modeling and virtual fitting technology," The Journal of The Textile Institute, pp. 1-15, 2025.

[9] Y. Dai and X. Yu, "Research on 3D reconstruction and digital protection of woodcarving works based on the combination of U-Net model and 6G network," Discover Applied Sciences, vol. 6, no. 12, pp. 668, 2024, doi: 10.1007/s42452-024-06406-y.

[10] M. Tacchetti, A. Chocontá-Piraquive, N. Quiceno Toro, and D. Papadopoulos, "Memorial reparation: Women's work of remembrance, repair and restoration in rural Colombia," Memory Studies, vol. 17, no. 6, pp. 1327-1345, 2023, doi: 10.1177/17506980231188482.

[11] Q. Yu and G. Zhu, "Digital Restoration and 3D Virtual Space Display of Hakka Cardigan Based on Optimization of Numerical Algorithm," Electronics, vol. 12, no. 20, pp. 4190, 2023, doi: 10.3390/electronics12204190.

[12] A. Shariq, A. Khan, A. M. Khan, M. Khurram, M. F. Umer, and M. S. Salam, "Image Processing Based Pattern Recognition and Computerized Embroidery Machine," Pakistan Journal of Engineering and Technology, vol. 5, no. 4, pp. 68-74, 2022, doi: 10.51846/vol5iss4pp68-74.

[13] A. Ibrahimi and M. Hessami, "Analysis of Herat embroidery patterns from the perspective of fractal geometry," Journal of Islamic Crafts, vol. 4, no. 2, pp. 1-12. https://sid.ir/paper/986525/en, 2021.

[14] Y. Zhang, H. Zhao, L. Qi, J. Zhang, and T. Zhang, "Research on the co-occurrence feature mining of the Qing Dynasty embroidery patterns based on temporal multilayer networks," Npj Heritage Science, vol. 13, no. 1, pp. 228, 2025, doi: 10.1038/s40494-025-01766-z.

[15] Y. Wang, M. F. Ramli, H. Song, and X. Li, "Exploring the Path of Cultural Sustainability for Traditional Costume Embroidery Patterns Based on Digital Generative Art," Cultura: International Journal of Philosophy of Culture and Axiology, vol. 21, no. 4, pp. 271-286. https://doi.org/10.70082/cijpca.v21i4.674, 2024.

[16] L. Yu, "Digital Sustainability of Intangible Cultural Heritage: The Example of the "Wu Leno" Weaving Technique in Suzhou, China," Sustainability, vol. 15, no. 12, pp. 9803, 2023, doi: 10.3390/su15129803.

[17] Y. Wang, W. Li, and Y. Zhang, "Mathematical Model Design of the Traditional Dress Recognition Algorithm Based on Digital Watermarking Technology," Mathematical Problems in Engineering, vol. 2022, no. 1, Art. no. 5230996, 2022, doi: 10.1155/2022/5230996.

[18] K. Meng, H. Li, Y. Shu, M. Chen, X. Han, and L. He, “Database construction and remodeling method on traditional Yi nationality patterns of China with GAN model,” Npj Heritage Science, vol. 13, no. 1, pp. 181, 2025, doi: 10.1038/s40494-025-01707-w.

[19] S. Sha, Y. Li, W. Wei, Y. Liu, C. Chi, X. Jiang, et al., “Image Classification and Restoration of Ancient Textiles Based on Convolutional Neural Network,” International Journal of Computational Intelligence Systems, vol. 17, no. 1, pp. 11, 2024, doi: 10.1007/s44196-023-00381-9.

[20] P. Kumar and V. Gupta, “Restoration of damaged artworks based on a generative adversarial network,” Multimedia Tools and Applications, vol. 82, no. 26, pp. 40967-40985, 2023, doi: 10.1007/s11042-023-15222-2.

[21] X. Han, Y. Wu, and R. Wan, “A Method for Style Transfer from Artistic Images Based on Depth Extraction Generative Adversarial Network,” Applied Sciences, vol. 13, no. 2, pp. 867, 2023, doi: 10.3390/app13020867.

[22] Z. Kazlacheva, J. Ilieva, P. Dineva, V. Stoykova, and Z. Zlatev, “Digital Color Images as a Tool for the Sustainable Use of Embroidery Elements from Folk Costumes,” Heritage, vol. 6, no. 8, pp. 5750-5778, 2023, doi: 10.3390/heritage6080303.